Thermal desorption–ion mobility spectrometry: A rapid sensor for the detection of cannabinoids and discrimination of *Cannabis sativa* L. chemotypes

María del Mar Contreras[a#], Natividad Jurado-Campos[a#], Carolina Sánchez-Carnerero Callado[b], Natalia Arroyo-Manzanares[a], Luis Fernández[c,d], Salvatore Casano[b], Santiago Marco[c,d], Lourdes Arce[a]* and Carlos Ferreiro-Vera[b]

[a]Department of Analytical Chemistry. Institute of Fine Chemistry and Nanochemistry, University of Córdoba, Campus de Rabanales, Marie Curie Annex Building, E-14071 Córdoba, Spain.

[b]Phytoplant Research S.L., The Science and Technology Park of Córdoba-Rabanales 21, Astronoma Cecilia Payne Street, Centauro Building, B-1, 14014. Córdoba, Spain.

[c]Department of Electronics and Biomedical Engineering, Universitat de Barcelona, Marti i Franquès 1, 08028-Barcelona, Spain.

[d]Signal and Information Processing for Sensing Systems, Institute for Bioengineering of Catalonia (IBEC), The Barcelona Institute of Science and Technology, Baldiri Reixac 10-12, 08028 Barcelona, Spain.

Corresponding author: *lourdes.arce@uco.es, Tel:+34-957-218-562, Fax:+34-957-218-614

[#]Both authors contribute equally

Abstract

Existing analytical techniques used for the determination of cannabinoids in *Cannabis sativa* L. (*Cannabis*) plants mostly rely on chromatography-based methods. As a rapid alternative for the direct analysis of them, thermal desorption (TD)-ion mobility spectrometry (IMS) was used for obtaining spectral fingerprints of single cannabinoids from *Cannabis* plant extracts and from plant residues on hands after their manipulation. The ionization source was ^{63}Ni, with automatic switchable polarity. Although in both ionization modes there were signals in the TD-IMS spectra of the plant extracts and residues that could be assigned to concrete cannabinoids and chemotypes, most of them could not be clearly distinguished. Alternatively, the global spectral data of the plant extracts and residues were pre-processed and then, using principal component analysis (PCA)-linear discriminant analysis (LDA), grouped in function of their chemotype in a more feasible way. Using this approach, the possibility of false positive responses was also studied analyzing other non-*Cannabis* plants and tobacco, which were clustered in a different group to those of *Cannabis*. Therefore, TD-IMS, as analytical tool, and PCA-LDA, as a strategy for data reduction and pattern recognition, can be applied for on-site chemotaxonomic discrimination of *Cannabis* varieties and detection of illegal marijuana since the IMS equipment is portable and the analysis time is highly short.

Keywords: *Cannabis sativa* L.; cannabinoids; chemometrics; chemotype; ion mobility spectrometry

1. Introduction

Cannabis sativa L. (*Cannabis*) (family *Cannabaceae*) is one of the most ancient domesticated crops. In some zones of the world, *Cannabis* has been mainly cultivated as fibre and grains source, while in other zones this plant have been also used as spiritual and recreational drug [1,2]. The vast majority of modern industrial hemp varieties are characterized by a low content of Δ^9-tetrahydrocannabinol (Δ^9-THC), the main psychoactive cannabinoid, and having cannabidiol (CBD), a non-psychoactive isomer of Δ^9-THC, as predominant cannabinoid. Based on the peaks ratio of Δ^9-THC, CBD and cannabinol (CBN), an oxidation product of Δ^9-THC, *Cannabis* has been generically subdivided into: fibre-type when ([Δ^9-THC]+[CBN])/[CBD] is <1 and drug-type (i.e. marijuana, marihuana, herbal *Cannabis* or *Cannabis*) when ([Δ^9-THC]+[CBN])/[CBD] is >1 [1]. However, this formula cannot be used for legal purposes while the content of Δ^9-THC is used for the discrimination of fibre and drug-types, being regulated on a national level and ranging from 0.2% in European Union countries to 1.0% in countries such as Switzerland, Uruguay and Colombia. Additionally, in last decades medicinal *Cannabis* varieties with different chemotypes have been selected [3], and some of these chemotypes are characterized for having different cannabinoids, such as cannabigerol (CBG), cannabidivarin (CBDV), and Δ^9-tetrahydrocannabivarin (Δ^9-THCV), than the ones considered in the previous formula. It is possible that in such cases the formula does not perfectly fit with the generic subdivision into fibre and drug-types. The scientific interest in both types of *Cannabis* (fibre-type and drug-type), as well as on chemotypes of medicinal varieties, is constantly growing, explained by the fact that: i) *Cannabis* is still the most widely cultivated, produced, trafficked and consumed drug worldwide, with approximately 183 million consumers in 2014 [4], ii) since 1990 the crop of hemp has been introduced or reintroduced in several countries to obtain fibre and grains [2,5], and

iii) it is increasingly being explored for medicinal applications and therapies, together with one of its main cannabinoids, CBD [2,6].

Cannabinoids are characteristic of the *Cannabis* genus and are composed of more than 120 terpenophenolic species [7]. In *Cannabis* plants these compounds are produced biosynthetically as their carboxylic acid forms (cannabinoid acids) [8]. In brief, cannabigerolic acid (CBGA) is formed by the condensation of the precursors geranyldiphosphate and olivetolic acid. Then, CBGA is transformed to Δ^9-tetrahydrocannabinolic acid (Δ^9-THCA), cannabidiolic acid (CBDA) or cannabichromenic acid (CBCA). Finally, CBG, Δ^9-THC, CBD, and cannabichromene (CBC) are generated by decarboxylation of the previous acidic forms during storage, through interaction with heat and light or when smoking [9,10]. Moreover, Δ^9-THC may be partly oxidized to CBN after harvesting and drying the plant material [1], or be transformed by isomerization to Δ^8-tetrahydrocannabinol (Δ^8-THC), which is an artefact not usually found in plant material [11]. Other minor cannabinoids, such as CBDV and Δ^9-THCV with a shorter *n*-propyl side chain instead of a *n*-pentyl group as the aforementioned ones [10], have been selected in some medicinal varieties for their higher contents, distinguishing them in new different chemotypes. Table S1 shows some physicochemical parameters of these compounds and their chemical structures.

For the analysis of *Cannabis* samples, forensic laboratories use colorimetric tests, but in some cases they can lead to false positive results in the presence of other plants [7]. Chromatographic techniques are commonly applied for this purpose, including thin layer chromatography (TLC), gas chromatography (GC) and liquid chromatography (LC). In particular, GC coupled to flame ionization detector (FID) or mass spectrometry (MS) are highly selective, but acidic forms of cannabinoids are decarboxylated into their neutral counterparts due to heating and the thermo-degradation (oxidation and isomerization) of

Δ^9-THC may also occur in the injector [1, 11–13]. Thus, a derivatization step, normally by silylation, is required to avoid the conversion of Δ^9-THCA into Δ^9-THC, making the analysis time longer. However, several reference methods for the determination of Δ^9-THC and the ratio [Δ^9-THC+CBN]/[CBD] were based on GC analysis [1,14]. These inconveniences could be solved using LC-MS. Nevertheless, GC- and LC-MS provide very reliable identification and selectivity, but they cannot readily be made portable for in-field measurements. Bear in mind, moreover, that the samples should be pretreated before being injected into the chromatographic system which is time-consuming and usually an error source. In this context, it seems plausible to apply sensors that enable the rapid screening and distinction of *Cannabis* types (fibre-type and drug-type) and chemotypes of medicinal varieties for both on-site drug control and quality control of vegetal raw material used by the pharmaceutical industry.

Ion mobility spectrometry (IMS) is a potential alternative because of its rapid analysis time, simplicity, sensitivity, and portability [15]. IMS has been used as a sensor to analyze drugs. Its use to detect Δ^9-THC in the positive ionization mode seems promising, while what happens in the negative ion mode is not known. However, some drawbacks were reported, such as poor selectivity and the existence of false-positive responses [15–17]. Moreover, most of these methods were tested using standards and no real samples [17–20].

Therefore, in this work a thermal-desorption (TD)-IMS was selected to obtain spectral fingerprints of *Cannabis* herbal samples, with and without pretreatment, in the positive and negative ionization modes. A chemometric strategy based on principal component analysis (PCA)-linear discriminant analysis (LDA) was then performed for the chemotyping of different *Cannabis* varieties to demonstrate the potential of TD-IMS for the screening of cannabinoids.

2. Material and methods

2.1 Plant material

A total of 33 *Cannabis* samples were used. Some of these samples were taken from plants of asexually propagated medicinal varieties registered by Phytoplant in the Community Plant Variety Office (CPVO) (http://cpvo.europa.eu/en) and identified with denomination proposals, while other samples were taken from plants of genotypes and hybrids, obtained as a result of an internal breeding program and identied with codes, and from plants of modern industrial hemp varieties identified with their denominations. The information about *Cannabis* plant materials is shown in Table 1.

Plant samples were obtained from the top of the plant at the optimal harvest point; about 30 cm containing both leaves and flowers (female inflorescences) were sampled for each plant, and then dried at 40 ºC for 72 hours in a forced ventilation oven (J. P. Selecta model Conterm 2000210, Barcelona, Spain). The stems were removed and the dried samples were ground until obtaining a semi-fine powder (passing through a 1 mm mesh sieve). A portion of approximately 1 g was placed into heat sealed pouches and stored at 4 ºC until analysis.

In order to evaluate potential interferences, five different kinds of non-*Cannabis* species (*Equisetum arvense*, *Matricaria chamomilla*, *Calendula officinalis*, *Papaver rhoeas*, and *Origanum vulgare*), as well as tobacco from two commercial different brands and aromatic pipe tobacco were purchased from local shops (Table 1). The dry plant materials were ground and stored as before.

2.2 Reagents

Cannabinoids standard compounds, deuterated cannabidiol (d3-CBD), CBDV, Δ^9-THCV, CBD, CBC, Δ^8-THC, Δ^9-THC, CBG and CBN, were purchased from THCPharm (Frankfurt, Germany). Their acidic forms, CBDA, CBGA and Δ^9-THCA were purchased from Cerilliant (Round Rock, Texas, USA). All standards were commercially acquired as solution at in methanol at 1000 mg L^{-1}. As commented before, Table S1 summarizes the characteristics of these cannabinoids.

HPLC grade *n*-hexane was obtained from Panreac (Barcelona, Spain), and trimethylchlorosilane (TMCS) as well as N,O-bis(trimethylsilyl)trifluoro-acetamide (BSTFA) reagents from Sigma-Aldrich (St. Louis, MO, USA). Purified nitrogen (N_2, 5.0) was supplied by Abelló Linde (Barcelona, Spain).

Stock and working solutions were stored at -18 °C. Working solutions were also prepared in hexane at different concentrations before analysis.

2.3 Plant extracts

Powdered plant materials (100 mg) were extracted with 5 mL of *n*-hexane, placed in an ultrasound bath for 20 min, and centrifuged for 5 min at 3000 rpm. Then, the supernatant containing cannabinoids was collected and stored at -18 ºC until analysis.

2.4 Instrumentation and software

2.4.1 IMS device

A handheld IMS (Gas Detector Array) with a thermal desorption (TD) unit (X-TOOL) (GDA-X) (Airsense Analytics GmbH, Germany) was employed. The TD-IMS consisted of two parts with the following dimensions: IMS device ~395 × 112 × 210 mm and the TD unit ~110 × 64 × 113 mm. For analyzes, samples were deposited on a wipe sampling pad (stainless steel coated with Teflon) and inserted in the tool tray. A scheme

of the GDA-X, including the wipe sampling pad, is shown in Figure S1a. IMS data were acquired in the positive and negative ionization modes using the WinMusterGDA software (version 1.2.6.12) (Figure S1b) from Airsense Analytics GmbH.

2.4.2 GC-MS equipment

An Agilent GC 7890B series (Agilent Technologies Inc, Santa Clara, CA, USA) equipped with a 7693 autosampler and a 5877B mass detector was used. The instrument was equipped with a Rxi-35Sil MS capillary column (15 m length, 0.25 mm internal diameter, film thicknes 0.25 μm) (Resteck, Bellefonte, PA, USA). The device was controlled by the software Agilent GC MassHunter Workstation 7.0 version.

2.5 TD-IMS analysis

For standards and plant extracts measurements, 6-24 μL (0.6-2.4 μg) of sample was carefully deposited on the centre of the wipe sampling pad, avoiding the diffusion of the liquid towards the peripheral zones of the fibre. Then, samples were heated at 60 °C for 4 min to eliminate the solvent. After this time, the wipe sampling pad was placed into the X-TOOL, and when it reached a temperature of 240 °C, the data were measured in both modes for about 20 seconds. Thus, once the analytes were desorbed, they were driven with atmospheric air (400 mL min^{-1}) until the ionization chamber. In this module, the compounds were ionized by a ^{63}Ni source, and the generated ions passed until the drift tube (6.29 cm length) through the shutter grid, which was open for 200 μs and operated at a constant temperature (60 °C) and at atmospheric pressure. The drift gas (clean air) flow was set at 200 mL min^{-1}. All these parameters are summarized in Table 2.

For the direct analysis of plant materials, the plant residues on fingers of laboratory staff were also analyzed. For that, they passed one finger over the inner surface of the

pouches, where the plants were stored, for 20 s. Consecutively, the fingers were rubbed on the surface of the wipe sampling pad in a circular manner for 20 s. Then, the measurements were carried out as before.

2.6 GC-MS analysis

The content of cannabinoids was evaluated by GC-MS analysis. For the simultaneous measure of neutral and acidic cannabinoids a derivatization process was carried out. Thus, a representative portion of the hexane extract mentioned in section 2.3 was transferred to a clean tube, evaporated to dryness and then derivatized with BSTFA:TMCS (98:2, v/v) at 37 ºC for 60 min. After cooling to room temperature, the samples were transferred to GC vials, which were recapped. The trimethylsilyl (TMS) derivatives were analyzed by GC-MS. The injector temperature was 250 ºC, with an injection volume of 1 µL in splitless mode and a carrier gas (He) flow rate of 2.5 mL/min. The temperature gradient started at 150 ºC, maintained 1 min and linearly increased at a rate of 50 ºC/min until 170 ºC, then it was linearly increased at 1 ºC/min until 177 ºC, increased again at 25 ºC/min until 230 ºC, and finally at 120 ºC/min until 300 ºC, which was held for 3 min. The MS interface temperature was set to 330 ºC. The internal standard employed was d3-CBD.

2.7 Chemometric analysis of the IMS data

As commented before, the GDA-X operated with automatic switchable polarity, obtaining ion mobility spectra in the positive and negative ionization modes (see Figure S1b). A spectrum was recorded every 1.5 s, approximately (including positive and negative polarity). The drift time and sample frequency were 30 ms and 30 kHz, respectively. The signals were pre-processed and a multivariate analysis was performed using the statistical software MATLAB (The Mathworks Inc., Natick, MA, USA, 2007) and PLS Toolbox 5.5 (Eigenvector Research, Inc., Manson, WA, USA).

The pre-processing of the positive and negative IMS data for each sample was performed individually. As an example, Figure S2 summarizes the main steps carried out using MATLAB. Firstly, the IMS data files (*.scm/*.nos) were converted to the format *.mat. Next, the pre-processing basically consisted of: 1) baseline correction, 2) smoothing with a Savitzky-Golay filtering, 3) spectra cutting for alignment in *y* axis and selection of relevant spectral data, and 4) transposition as well as spectra concatenation. Then, baseline was corrected selecting the first 150 points (1:150) and the last 295 (600:895) from each spectrum, where no peaks were found, and fitting to a 4^{th} order polynomial. The noise reduction was performed using a second order Savitzky-Golay filter, with a window width of 9. Afterwards, the spectra were cut, their size matched for all samples and the reactant ion peak (RIP) removed. This also included that the sample data were cut from the scan where the signals of the samples began to appear to the end of the registered scans. Globally, this means that six spectra were taken in *y* axis and from point 270 to the end in *x* axis. Finally, the rows were transposed, and the concatenation of the spectra was carried out. The dimensions of the concatenated data was 1 × 3756.

Once the pre-processing was performed, each concatenated spectrum was arranged consecutively to obtain the data matrices and to build the chemometric models. The samples and classes, according to their psychoactivity and chemotype, included in the models are in Table 1. Firstly, in order to detect outliers, individual PCAs using auto-scaled data were carried out for each group of samples. A statistical confidence region provided by the software was used as an aid in the detection of outliers. This confidence region is based on Hotelling's T^2-test, which is a multivariate version of Student's t-test. The confidence limit was 95%. Later, a non-supervised PCA analysis using auto-scaled data was employed for dimensionality reduction and extraction of the most relevant information. In all cases, the number of principal components accounted for a cumulative

variance of 90%. Finally, LDA was used to incorporate class information into the model and find directions to maximize the class separation [21].

3. Results and discussion

3.1 Analysis by GC-MS

As commented before, GC is usually applied in several reference methods for the determination of cannabinoids. In this work, GC-MS was firstly used to determine the ratio of ([Δ^9-THC]+[CBN])/[CBD] in the plant samples. Moreover, the rest of cannabinoids, Δ^9-THCA, CBDA, CBGA, CBG, Δ^9-THCV, CBDV, Δ^8-THC, and CBC, were also determined to group in chemotypes the varieties of plants according to the major ones. This information is summarized in Table 1.

3.2 Optimization of the IMS methodology

Firstly, an UV-IMS was tested for the detection of cannabinoids standards. The UV-IMS employed was described by Criado-García et al. [22]. Although different incubation times and temperatures were tested using an oven (255 ºC) (HP 5890, Agilent Technologies) and a thermo-reactor (80-200 ºC) (Velp Scientific, Usmate, Italia) that were coupled to the UV-IMS as described Garrido-Delgado et al. [23], the cannabinoids could not be detected using this methodology. So, a TD-IMS with a ^{63}Ni ionization source was selected for these purposes.

The conditions related to the analysis of cannabinoids by using a TD-IMS were assessed. Firstly, the influence of the solvent (hexane) was evaluated immediately after smearing on the surface of the wipe sampling pad. Although hexane (672.5 kJ/mol) has a lower proton affinity than water (691.0 kJ/mol) [24], several signals that may interfere with the compounds of interest were detected. An example is shown in Figure S3, and as

it can be seen, using hexane the CBC signal was not observed and only hexane signals were seen. However, CBC signals appear in the absence of hexane. Thus, hexane was removed to avoid a loss of sensitivity and contamination of the detector. Derivation agents were also avoided for the same reasons. Moreover, the influence of the sample volume (6, 12, and 24 µL) deposited on the pad was studied using cannabinoids standards at 100 mg L^{-1}. Not surprisingly, a volume of 12 µL was chosen, achieving more intense signals than that obtained when using 6 µL. However, a larger sample volume was not used due to the difficulty getting a centered drop in the wipe pad, which affects to the volatilization efficiency, and so the detected signal. In the case of the analysis of cannabinoids residues on fingers, a contact during 20 s with the pad was employed to ensure that the compounds were homogeneously retained.

Once the analytical methodology was well established, all the commercial cannabinoids standards were analyzed. Table 3 lists the reduced mobilities values (K_0) of the main signals (markers) detected for each compound in the positive and negative ionization modes during the analysis (drift time scans). The K_0 values of some of these peak signals agreed well with those previously reported in literature, i.e. the protonated monomer of CBD (1.08 ± 0.02 cm^2 V^{-1} s^{-1}) [18] and Δ^9-THC (1.05 ± 0.0004 and 1.06 cm^2 V^{-1} s^{-1}) [15,18,19]. In these previous studies, only the K_0 value of the most intense peak was pointed out in a drift time measurement using TD-IMS [15], while other used electrospray ionization, a soft volatilization/ionization source [18]. Moreover, nicotinamide (with a high proton affinity, 918.3 kJ/mol) was employed as an internal calibrant using TD-IMS in the positive ionization mode [15,19]. This means that only molecules with higher proton affinity in the vapor phase were protonated and detected, increasing the selectivity of the analysis [15], but it reduces the number of the markers detected compared to those found in the present work. Thus, it should be noted that the

283 markers reported in the Table 3 enrich the literature with new data about the studied
284 cannabinoids in both positive and negative ionization modes.

285 The mobility spectra profiles obtained for each cannabinoid prepared at the same
286 concentration (100 mg L^{-1}) in the positive and negative ionization modes during the
287 analysis are depicted in Figure S4 and S5, respectively. In the positive mode, the profiles
288 of some compounds presented different signals, which enable their differentiation, e.g.,
289 CBDA (only two signals appear at 1.09 and 1.42 cm^2 V^{-1} s^{-1}), CBG (signal at 1.92 cm^2
290 V^{-1} s^{-1}), Δ^9-THCV (signal at 1.16 cm^2 V^{-1} s^{-1}), CBDV (signals at 1.18 and 1.71 cm^2 V^{-1} s^{-1}) and CBGA (the signals at 1.92 or 1.16/1.18 cm^2 V^{-1} s^{-1} does not appear). However, Δ^9-
292 THCA, Δ^8-THC, Δ^9-THC, CBD, CBC, and CBN gave similar profiles, sharing a signal
293 with K_0 1.08 cm^2 V^{-1} s^{-1} (Δ^9-THCA, Δ^8-THC and Δ^9-THC) and 1.09 cm^2 V^{-1} s^{-1} (CBD,
294 CBC and CBN), but with changes in intensity. In negative mode, some of the studied
295 compounds can be also differentiated visually based on their fingerprints, e.g., CBD,
296 CBG, THCV, CBDV, CBGA and CBC. However, Δ^9-THCA, Δ^9-THC, CBDA, Δ^8-THC
297 and CBN presented a signal closer to K_0 1.01/1.02 cm^2 V^{-1} s^{-1} whose intensity varied
298 depending on the compound. The above suggests that the direct differentiation of the
299 cannabinoids through their TD-IMS fingerprints is possible, however, it is a difficult task
300 especially for those aforementioned compounds that shares some common signals. Then,
301 before the analysis of more complex samples, i.e. *Cannabis* extracts and plant materials,
302 a chemometric study of the global spectra of the cannabinoids standards was carried out
303 employing positive and negative data recorded by TD-IMS as well as the positive and
304 negative data arranged together. For that, the aforementioned data of the cannabinoids
305 were pre-processed following the steps summarized in Material and Methods, and a PCA
306 was performed to assess the applicability of the strategy.

307 The cumulative percentage of the PCA in the positive, negative, and positive +
308 negative ionization modes were 91.03% (five components), 92.85% (six components),
309 and 90.95% (six components) for an input dataset of 22 samples, i.e. two measurements
310 of each individual cannabinoid standard. As an example, Figure 1 shows the most
311 representative score plots of the PCAs, respectively. In the positive mode, with three
312 components, Δ^9-THCV, CBDV, CBDA, CBGA and CBG were clustered separately (see
313 Figure 1A). Additionally, with five components (PC1 *vs* PC5), CBC could be also
314 separated, while Δ^9-THCA was slightly separated from Δ^9-THC (see Figure 1B).
315 However, it is difficult to differentiate CBC from Δ^9-THCA, Δ^9-THC or Δ^8-THC, by
316 simply visual inspection (see Figure S4). So, the need of chemometric data treatment can
317 be highlighted with this example. In the negative mode, Δ^9-THCV, CBDV, CBD and
318 CBG were grouped separately in the first two components (see Figure 1C), while Δ^8-THC
319 appeared in an extreme of the plot and separated using five components (see Figure 1D).
320 Notice that CBD was not well separated in the positive ionization mode. So, the analysis
321 in the positive ionization mode, which is the commonest mode used in IMS, can be
322 complemented with the negative one. The PCA of the combined data positive + negative
323 needed more components, with similar results than the PCAs of the individual IMS
324 polarities. Anyway, this strategy could be useful if the analysis using individual positive
325 or negative data fail in clustering some compounds.

326 **3.3 Plant extracts**

327 **3.3.1 Evaluation of the TD-IMS spectra**

328 A common solid-liquid extraction method using *n*-hexane was applied to extract the
329 cannabinoids (see section 2.3). The extracts were firstly analyzed by GC-MS to define
330 *Cannabis* chemotypes based on their psychoactivity and the major cannabinoids groups
331 present in the plants (Table 1), as commented before.

Secondly, the extracts were checked by TD-IMS to correlate all the information. Figure 2 depicts examples of TD-IMS spectra of the different *Cannabis* chemotypes in the positive and negative ionization modes. In the positive ionization mode, the spectra of the extracts showed different profiles, but shared some common signals, e.g., at K_0 1.38-1.39 $cm^2\ V^{-1}\ s^{-1}$ (see Figures 2A1-A6). Some signals could be assigned to the presence of concrete cannabinoids by visual inspection of the spectra. As an example, peaks with K_0 close to 1.09 (e.g., chemotype 1), 1.18 (e.g., chemotype 2), 1.08 (e.g., chemotype 5) and 1.16 $cm^2\ V^{-1}\ s^{-1}$ are related to CBD/CBDA, CBDV, Δ^9-THC/Δ^9-THCA and Δ^9-THCV, respectively. In addition, the appearance of two peaks at K_0 1.05 and 1.10 $cm^2\ V^{-1}\ s^{-1}$ indicated the presence of CBGA and/or CBG. Nevertheless, the differentiation of the chemotypes using the positive ionization mode in this way is a difficult task due to the low peak resolution provided by the TD-IMS. As an example, there were peaks with shoulders not clearly resolved and wide peaks, which could be formed by several similar signals (e.g. at K_0 1.72, 1.68, 1.38 $cm^2\ V^{-1}\ s^{-1}$). Moreover, chemotype 1 and chemotype 6 shared the main peaks signals.

Generally, in the negative ionization mode the signal peaks showed lower intensities (see Figures 2B1-B6) than those obtained in the positive ionization mode (see Figures 2A1-A6). Similarly, the studied chemotypes gave different TD-IMS profiles and some peaks could be assigned to concrete cannabinoids.

To evaluate the possibility of obtaining false positive results, other plant materials were extracted with hexane and analyzed by TD-IMS: *Equisetum arvense* (*Equisetaceae*), *Matricaria chamomilla* (*Asteraceae*), *Calendula officinalis* (*Asteraceae*), *Papaver rhoeas* (*Papaveraceae*), and *Origanum vulgare* (*Lamiaceae*). Neither of these species contains cannabinoids. On the contrary, some of them contain terpenes, such as α-pinene, β-

pinene, myrcene and limonene [25–27], which are also present in *Cannabis* [28]. These volatiles have K_0 values between 1.26 and 1.28 ($cm^2\ V^{-1}\ s^{-1}$) [28,29]. Moreover, tobacco is usually smoked mixed with *Cannabis* in Europe [15]. Therefore, tobacco was also extracted and analyzed in order to evaluate the potential inferences of nicotine (K_0, 1.54 $cm^2\ V^{-1}\ s^{-1}$, [30]) and other components. The IMS spectra of these plants (Figure S6) and tobacco (Figure 3) were clearly different from both standards and *Cannabis* plants extracts. Although there were some common signals between these extracts, *Cannabis* plants extracts and/or cannabinoids standards, the characteristic signal of Δ^9-THC/Δ^9-THCA at K_0 1.08 $cm^2\ V^{-1}\ s^{-1}$ (positive ionization mode) were not found after subtraction of the blanks. In the negative ionization mode, the extracts of these plants presented TD-IMS profiles with low intensity signals, except *M. chamomilla*, and they were clearly different to those of *Cannabis*. There was also no presence of a signal at K_0 1.01 $cm^2\ V^{-1}\ s^{-1}$, characteristic of Δ^9-THC/Δ^9-THCA; reaffirming the results obtained in the positive ionization mode.

3.3.2 Multivariate data analysis

Due to the difficulty to differentiate *Cannabis* chemotypes by the visual inspection of the TD-IMS spectra, a chemometric study based on PCA-LDA [21] was performed after the pre-processing of the spectral fingerprint data, as for standards.

Our results showed that the extracts were grouped properly in different clusters according to the previous defined chemotypes, psychoactivity and major cannabinoids groups, in each ionization mode. Some examples are illustrated in Figure 4 for psychoactivity (A1) and major cannabinoids (B2) chemotypes and for positive (A1) and negative (B2) mode. Moreover, the aforementioned plants and tobacco were also extracted and analyzed by TD-IMS and PCA-LDA to check the potential of the methodology for *Cannabis* discrimination. In this way, non-*Cannabis* plants (including

tobacco) were clustered in a different group (see some examples in Figures 4A2 and B1). Compared to other IMS methodologies, Sonnberg et al. [15] found that some compounds from non-cannabinoids plants could be misinterpreted as Δ^9-THC because of a partial peak overlapping of signals at a similar drift time. An algorithm based on the inverse of the second derivative should be use to minimize the low selectivity of the TD-IMS. When using ESI-IMS, Kanu et al. [18] used the conditional reduced mobility (combination of reduced mobility and the width-at-half-height of a peak) to differentiate between real drugs peaks from those of false-positive peaks with similar K_0 values. Another study applied GC-FID to determine terpenoids and cannabinoids in ethanolic extracts of *Cannabis* plants and PCA for chemotaxonomic purposes, but the medium Δ^9-THC varieties were not well separated [8]. So, the methodology presented here can be used as a faster screening tool to complement GC-MS analysis, being able to discriminate *Cannabis* varieties from other plant species, including tobacco.

3.4 Residues of plants on fingers

3.4.1 Evaluation of the TD-IMS spectra

The direct measurement of plants residues on fingers, after being in contact with *Cannabis* plants, was also evaluated since this strategy is faster and can be applied on-site, not only for chemotyping but also for drug control. In fact, the most common way of *Cannabis* consumption is smoking, marijuana and hashish being manipulated to make cigarettes.

In the positive ionization mode, the spectra obtained show similar characteristic signals to those for hexane extracts, with some slight shifts, and a higher intensity (Figures 5A1-A6). On the contrary, in the negative ionization mode the spectra of the plants were more complex (see Figures 5B1-B6) than those observed after extraction with *n*-hexane,

406 indicating the potential detection of other polar phytochemicals. This could be explained
407 by the fact that *n*-hexane is a non-polar solvent. In these spectra, peaks with K_0 values at
408 1.01, 1.02, 1.08, and 1.27 $cm^2\ V^{-1}\ s^{-1}$ could be related to the presence of Δ^9-THCA and
409 Δ^9-THC, CBDA and CBD, CBDV, as well as CBGA, respectively (Figure 5 and Table
410 3).

411 When non-*Cannabis* plants (Figure S7) and tobacco (Figure 3) were evaluated, the
412 TD-IMS spectra in both modes were clearly different from those of cannabinoids
413 standards and *Cannabis* plants as before. As observed for *Cannabis* plants, the spectral
414 fingerprints were more complex than those of the hexane extracts. Moreover, in the
415 positive ionization mode a peak with K_0 close to 1.54 $cm^2\ V^{-1}\ s^{-1}$ was detected in tobacco
416 samples (Figure 3), which could be assigned to nicotine according to literature [30].

417 Despite the conclusions obtained throught the direct inspection of spectra, a deeper
418 and objective chemometric data treatment is necessary for the proper chemotyping of the
419 plants using TD-IMS.

420 **3.4.2 Multivariate data analysis**

421 A second strategy consisted of using PCA-LDA to discriminate *Cannabis*
422 chemotypes based on the direct measurement of the plant material by TD-IMS. Figure 6
423 summarizes some examples of the groups clustered in each ionization mode using PCA-
424 LDA; i.e. the plants could be separated in three and five groups according to the pre-
425 established chemotypes, i.e. psychoactivity (Figures 6A1) and major cannabinoids groups
426 (Figures 6B2), respectively. Moreover, when non-*Cannabis* plants were analyzed, they
427 were grouped in a separated cluster (Figures 6A2 and 6B1). However, using the positive
428 TD-IMS fingerprints, a partial overlapping of the chemotypes 2
429 (CBD+CBDA/CBDV+CBDVA) and 5 (Δ^9-THC+Δ^9-THCA) was observed (Figure 6A2).

Anyway, these strategies can be used for the detection of cannabinoids and the discrimination of *Cannabis* chemotypes, without the requirement of a pre-extraction method and so in a faster way than other methodologies, e.g., GC-FID [8], ESI coupled to Fourier transform ion cyclotron resonance MS [7], nuclear magnetic resonance and high performance TLC [31,32].

4. Conclusions

On the basis of these results, the methodology based on TD-IMS can be used to detect cannabinoids in the positive and negative ionization modes. These data combined with PCA-LDA as chemometric strategy was useful for the discrimination of *Cannabis* chemotypes after hexane extraction. Moreover, samples of different *Cannabis* plants could be also clustered in different chemotypes after the direct measurement of plant material as residue on fingers, making the analysis faster (< 2 min) and with applicability for on-site measurements, making this technical tool particularly attractive for *Cannabis* breeders. Potentially interfering non-*Cannabis* plants were measured, showing different TD-IMS fingerprint profiles than those of *Cannabis* plants, being clustered in a different group when using PCA-LDA. Thus, further studies are required to test the methodology on site for illegal marijuana handling through the detection of residues on hands of consumers.

Acknowledgements

The authors acknowledge support from the Government of Spain (DGICyT Project CTQ2014-52939R). N.A.M. thanks the Ministry of Economy and Competitiveness (MINECO) of the Spanish Government for a Juan de la Cierva post-doctoral contract (FJCI-2014-20321). N.J.C. wishes to thank the Spanish Ministry of Education, Culture and Sport for award of a FPU pre-doctoral grant.

References

[1] United Nations Office on Drugs and Crime, Recommended methods for the identification and analysis of cannabis and cannabis products, United Nations, New York, 2009.

[2] J. Cherney, E. Small, Industrial Hemp in North America: Production, Politics and Potential, Agronomy 6 (2016) 58.

[3] E. P. M. de Meijer, K. M. Hammond, The inheritance of chemical phenotype in *Cannabis sativa* L. (V): regulation of the propyl-/pentyl cannabinoid ratio, completion of a genetic model, Euphytica 210 (2016) 291–307.

[4] United Nations Office on Drugs and Crime, World Drug Report 2016. Cannabis, 2016.

[5] K. Tang, P.C. Struik, X. Yin, C. Thouminot, M. Bjelková, V. Stramkale, et al., Comparing hemp (*Cannabis sativa* L.) cultivars for dual-purpose production under contrasting environments, Ind. Crops Prod. 87 (2016) 33–44.

[6] J. Fike, Industrial Hemp: renewed opportunities for an ancient crop, CRC. Crit. Rev. Plant Sci. 35 (2016) 406–424.

[7] I.R. Nascimento, H.B. Costa, L.M. Souza, L.C. Soprani, B.B. Merlo, W. Romão, Chemical identification of cannabinoids in street marijuana samples using electrospray ionization FT-ICR mass spectrometry, Anal. Methods. 7 (2015) 1415–1424.

[8] J.T. Fischedick, A. Hazekamp, T. Erkelens, Y.H. Choi, R. Verpoorte, Metabolic fingerprinting of *Cannabis sativa* L., cannabinoids and terpenoids for chemotaxonomic and drug standardization purposes, Phytochemistry. 71 (2010) 2058–2073.

[9] N. Happyana, S. Agnolet, R. Muntendam, A. Van Dam, B. Schneider, O. Kayser, Analysis of cannabinoids in laser-microdissected trichomes of medicinal Cannabis sativa using LCMS and cryogenic NMR, Phytochemistry. 87 (2013) 51–59.

[10] A. Tubaro, A. Giangaspero, S. Sosa, R. Negri, G. Grassi, S. Casano, et al., Comparative topical anti-inflammatory activity of cannabinoids and cannabivarins, Fitoterapia. 81 (2010) 816–819.

[11] B. De Backer, B. Debrus, P. Lebrun, L. Theunis, N. Dubois, L. Decock, et al., Innovative development and validation of an HPLC/DAD method for the qualitative and quantitative determination of major cannabinoids in cannabis plant material, J. Chromatogr. B Anal. Technol. Biomed. Life Sci. 877 (2009) 4115–4124.

[12] A. Hazekamp, A. Peltenburg, R. Verpoorte, C. Giroud, Chromatographic and Spectroscopic Data of Cannabinoids from *Cannabis sativa* L., J. Liq. Chromatogr. Relat. Technol. 28 (2005) 2361–2382.

[13] J. Mazina, A. Spiljova, M. Vaher, M. Kaljurand, M. Kulp, A rapid capillary electrophoresis method with LED-induced native fluorescence detection for the analysis of cannabinoids in oral fluid, Anal. Methods. 7 (2015) 7741–7747.

[14] Commission Regulation (EEC) No 421/86 of 25 February 1986 amending Regulation (EEC) No 771/74 and Regulation (EEC) No 2188/84 by prescribing a Community method for the quantitative determination of tetrahydrocannabinol in hemp.

[15] S. Sonnberg, S. Armenta, S. Garrigues, M. de la Guardia, Detection of tetrahydrocannabinol residues on hands by ion-mobility spectrometry (IMS). Correlation of IMS data with saliva analysis, Anal. Bioanal. Chem. 407 (2015) 5999–6008.

[16] C. Fuche, A. Gond, D. Collot, C. Faget, The use of IMS and GC/IMS for analysis of saliva, IJIMS. (2001) 20–25.

[17] A.B. Kanu, H.H. Hill, Identity confirmation of drugs and explosives in ion mobility spectrometry using a secondary drift gas, Talanta 73 (2007) 692–699.

[18] A.B. Kanu, A. Leal, Identity Efficiency for High-Performance Ambient Pressure Ion Mobility Spectrometry, Anal. Chem. 88 (2016) 3058–3066.

[19] J.R. Verkouteren, J.L. Staymates, Reliability of ion mobility spectrometry for qualitative analysis of complex, multicomponent illicit drug samples, Forensic Sci. Int. 206 (2011) 190–196.

[20] Y. Mohsen, N. Gharbi, A. Lenouvel, C. Guignard, Detection of d9-tetrahydrocannabinol, methamphetamine and amphetamine in air at low ppb level using a field asymmetric ion mobility spectrometry microchip sensor, Procedia Eng. 87 (2014) 536–539.

[21] R. Garrido-Delgado, L. Arce, A. V. Guamán, A. Pardo, S. Marco, M. Valcárcel, Direct coupling of a gas–liquid separator to an ion mobility spectrometer for the classification of different white wines using chemometrics tools, Talanta 84 (2011) 471–479.

[22] L. Criado- García, N. Almofti, L. Arce, Photoionization-ion mobility spectrometer for non-targeted screening analysis or for targeted analysis coupling a Tenax TA column, Sensors Actuators B Chem. 235 (2016) 370–377.

[23] R. Garrido-Delgado, L. Arce, C.C. Pérez-Marín, M. Valcárcel, Use of ion mobility spectroscopy with an ultraviolet ionization source as a vanguard screening system for the detection and determination of acetone in urine as a biomarker for cow and human diseases, Talanta 78 (2009) 863–868.

[24] N. Sato, K. Sekimoto, M. Takayama, Ionization capabilities of hydronium ions and high electric fields produced by atmospheric pressure corona discharge, Mass Spectrom. 5 (2017) S0067–S0067.

530 [25] A.J. Karamanos, D.E.K. Sotiropoulou, Field studies of nitrogen application on
531 Greek oregano (*Origanum vulgare* ssp. hirtum (Link) Ietswaart) essential oil
532 during two cultivation seasons, Ind. Crops Prod. 46 (2013) 246–252.

533 [26] O.O. Okoh, A.P. Sadimenko, O.T. Asekun, A.J. Afolayan, The effects of drying
534 on the chemical components of essential oils of *Calendula officinalis* L., African
535 J. Biotechnol. 7 (2008) 1500–1502.

536 [27] M.H.H. Roby, M.A. Sarhan, K.A.H. Selim, K.I. Khalel, Antioxidant and
537 antimicrobial activities of essential oil and extracts of fennel (*Foeniculum vulgare*
538 L.) and chamomile (M*atricaria chamomilla* L.), Ind. Crops Prod. 44 (2013) 437–
539 445.

540 [28] H. Lai, P. Guerra, M. Joshi, J.R. Almirall, Analysis of volatile components of drugs
541 and explosives by solid phase microextraction-ion mobility spectrometry, J. Sep.
542 Sci. 31 (2008) 402–412.

543 [29] H. Lai, I. Corbin, J.R. Almirall, Headspace sampling and detection of cocaine,
544 MDMA, and marijuana via volatile markers in the presence of potential
545 interferences by solid phase microextraction-ion mobility spectrometry (SPME-
546 IMS), Anal. Bioanal. Chem. 392 (2008) 105–113.

547 [30] M.L. Ochoa, P.B. Harrington, Detection of methamphetamine in the presence of
548 nicotine using in situ chemical derivatization and ion mobility spectrometry, Anal.
549 Chem. 76 (2004) 985–991.

550 [31] C. Citti, D. Braghiroli, M.A. Vandelli, G. Cannazza, Pharmaceutical and
551 biomedical analysis of cannabinoids: A critical review, J. Pharm. Biomed. Anal.
552 147 (2018) 565–579.

553 [32] F. Fowler, B. Voyer, M. Marino, J. Finzel, M. Veltri, N.M. Wachter, et al., Rapid
554 screening and quantification of synthetic cannabinoids in herbal products with
555 NMR spectroscopic methods, Anal. Methods. 7 (2015) 7907–7916.

Figure captions

Figure 1. Representative PCAs score plots of the cannabinoids fingerprints: (A and B) positive, (C and D) negative modes.

Figure 2. Spectra of *Cannabis sativa* L. plants extracts obtained by thermal desorption-ion mobility spectrometry in the positive (A1-A6) and negative (B1-B6) ionization modes. The chemotypes are defined in Table 1. The arrows highlight the main characteristic signals of the chemotypes.

Figure 3. Spectra of tobacco extracts in the positive (A1-A3) and negative ionization modes (B1-B3), and spectra of tobacco residues on fingers in the positive (C1-C3) and negative ionization modes (D1-D3).

Figure 4. PCA-LDA plots for positive (A1-A2) and negative (B1-B2) spectra of *Cannabis sativa* L. and non-*Cannabis* plants extracts. The chemotypes are defined in Table 1.

Figure 5. Spectra of *Cannabis sativa* L. plants residues on fingers obtained by thermal desorption-ion mobility spectrometry in the positive (A1-A6) and negative (B1-B6) ionization modes. The chemotypes are defined in Table 1. The arrows highlight the main characteristic signals of the chemotypes.

Figure 6. PCA-LDA plots for positive (A1-A2) and negative (B1-B2) spectra of *Cannabis sativa* L. and non-*Cannabis* plants residues on fingers. The chemotypes are defined in Table 1.

581 Figure 1.

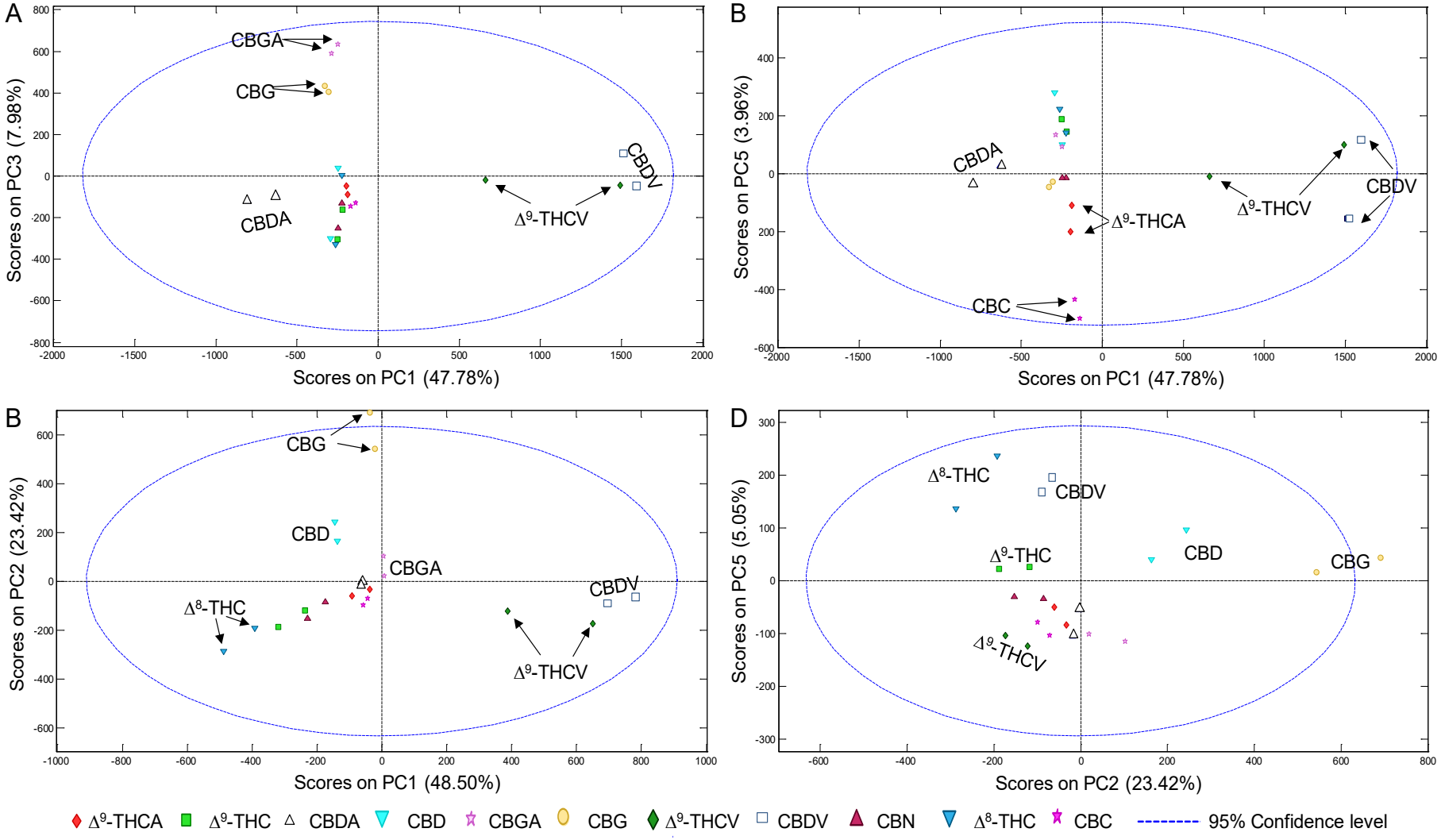

582
583

584 Figure 2.

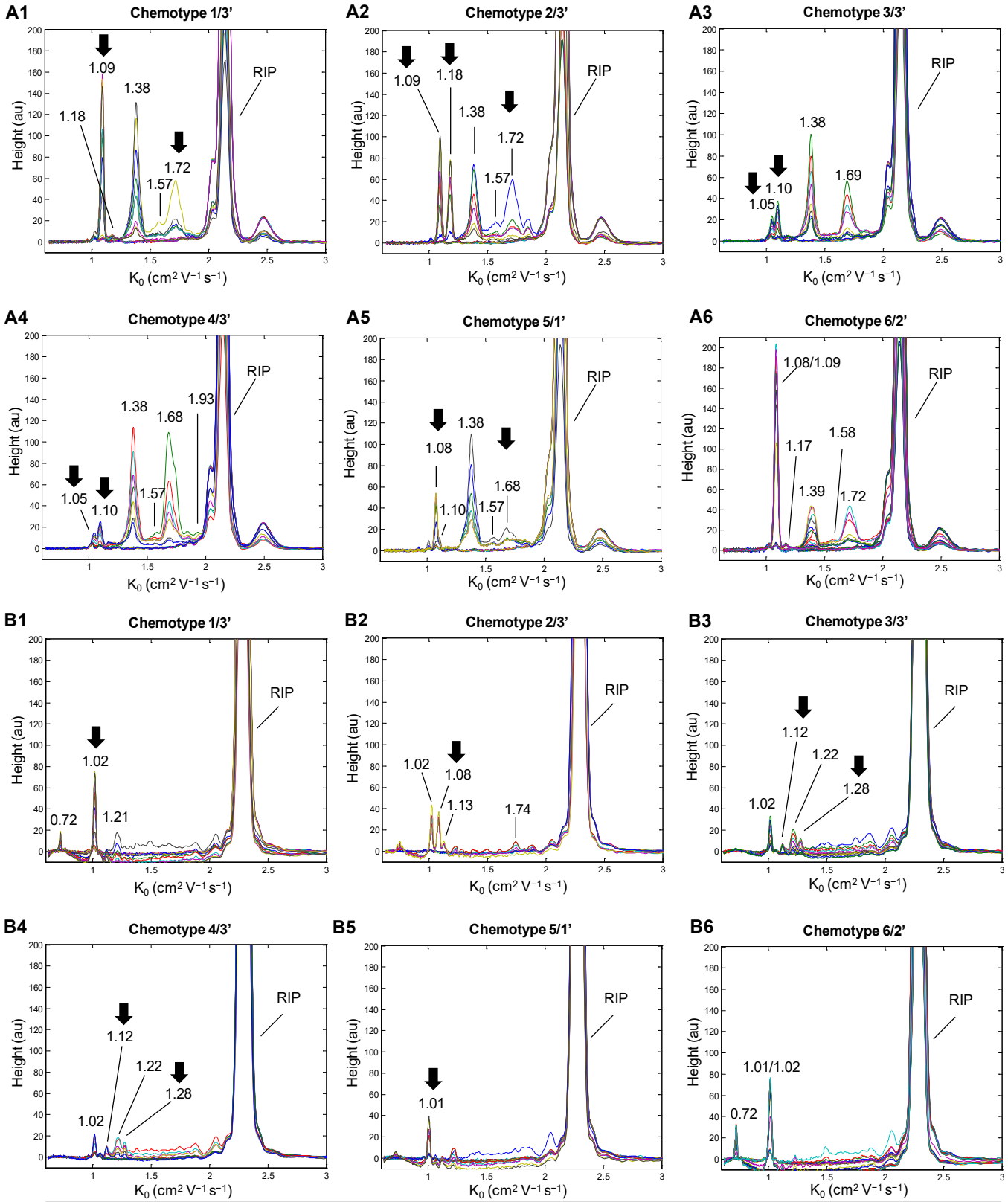

585 Chemotypes:
Based on the major cannabinoids groups: CBD+CBDA (1), CBD+CBDA/CBDV+CBDVA (2), CBD+CBDA/CBG+CBGA (3), CBG+CBGA (4), Δ^9-THC+Δ^9-THCA (5), and CBD+CBDA/Δ^9-THC+Δ^9-THCA (6).
Based on the psychoactivity: ([Δ^9-THC]+[CBN]) > [CBD] (1'), ([Δ^9-THC]+[CBN]) ≈ [CBD] (2'), ([Δ^9-THC]+[CBN]) < [CBD] (3').

586 Figure 3.

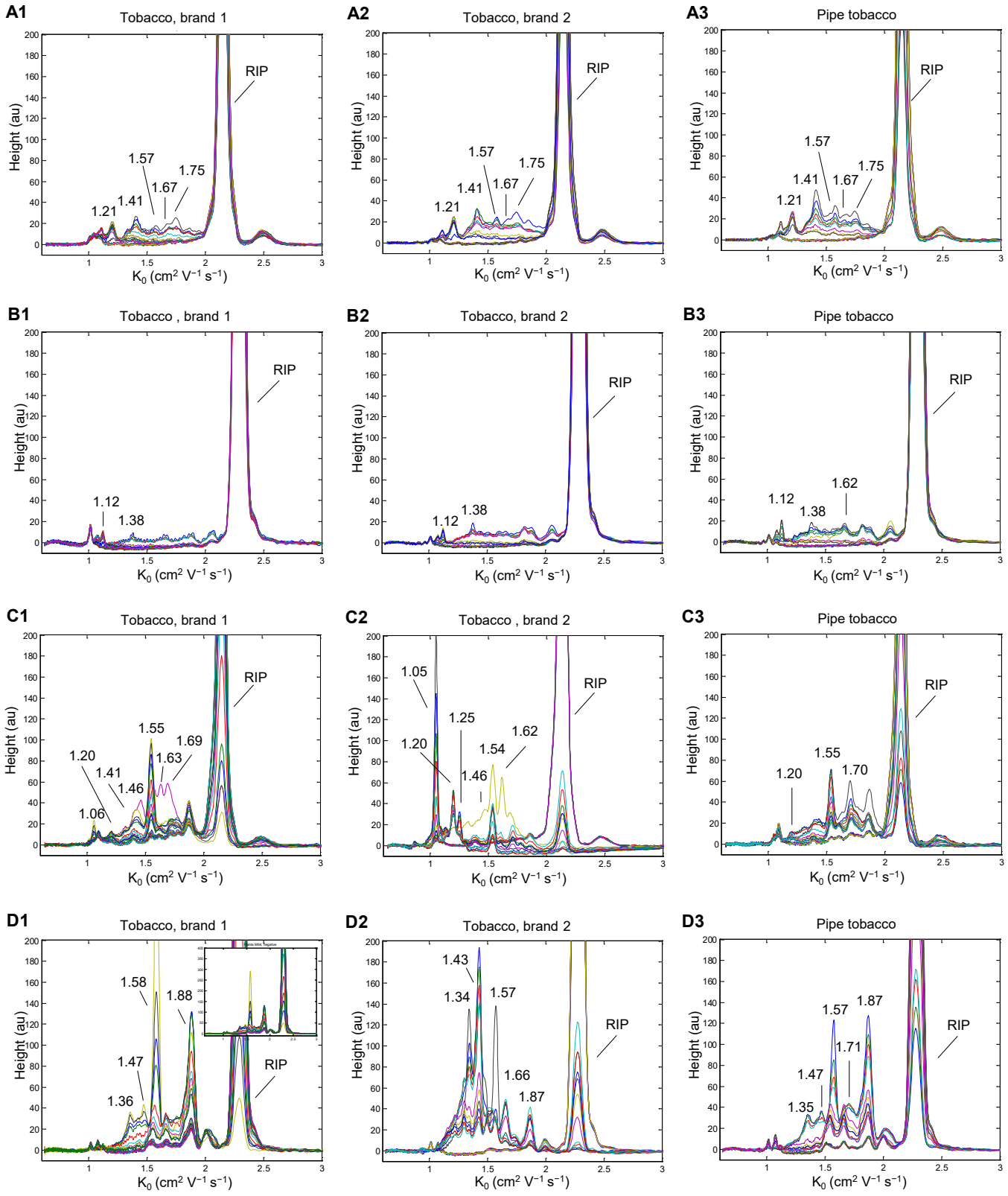

587

588

589 Figure 4.

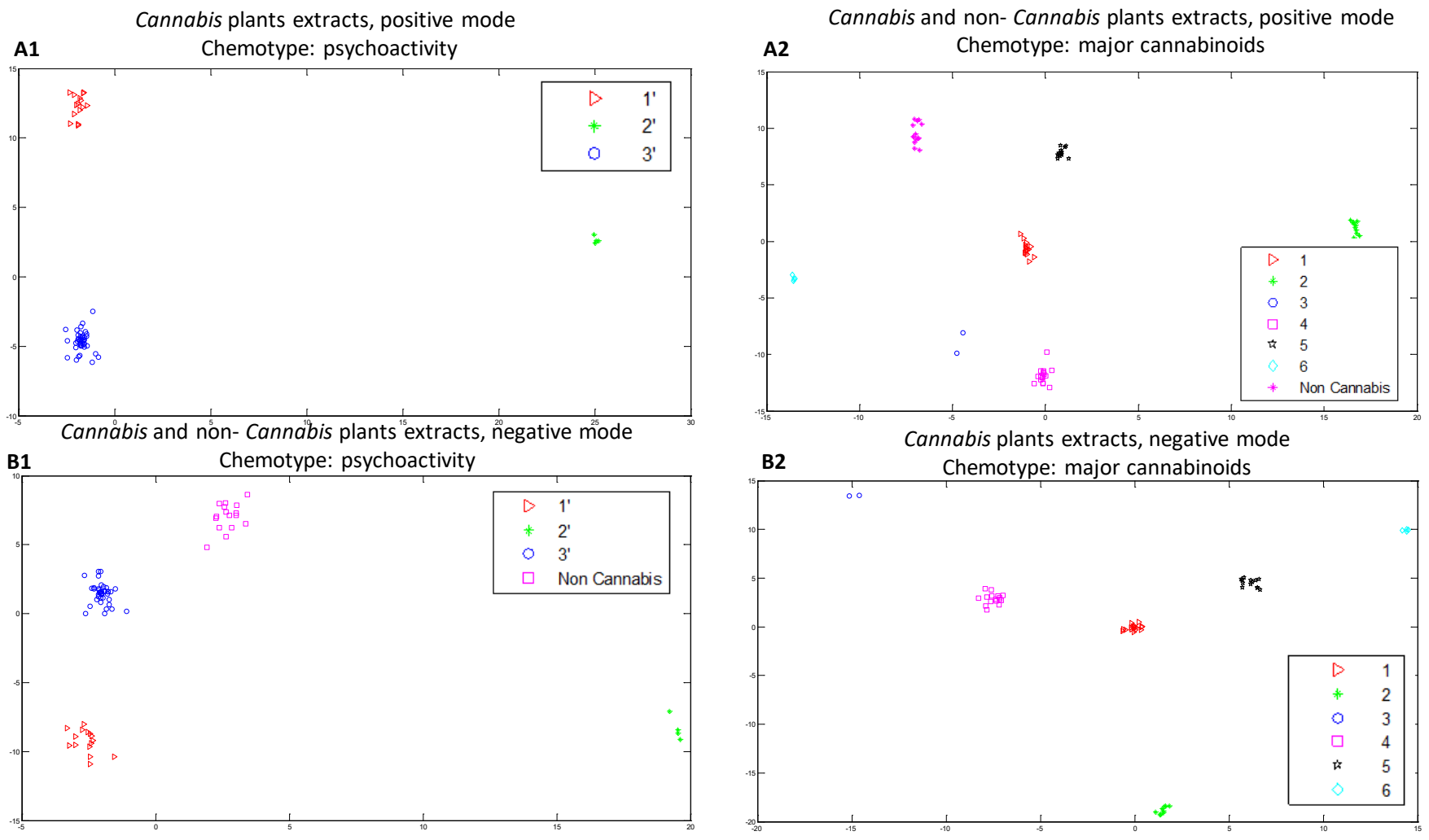

590

591 Figure 5.

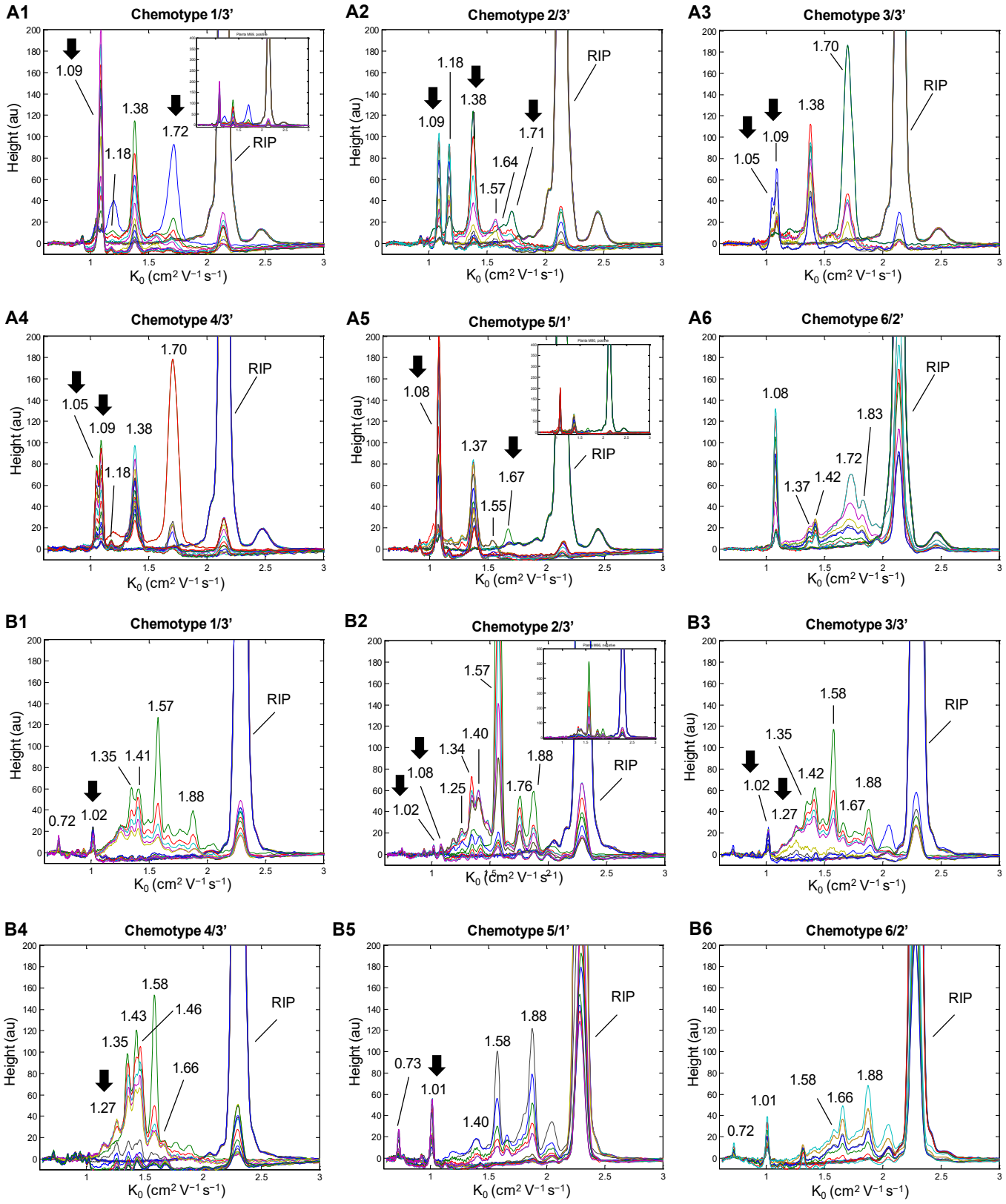

Chemotypes:
Based on the major cannabinoids groups: CBD+CBDA (1), CBD+CBDA/CBDV+CBDVA (2), CBD+CBDA/CBG+CBGA (3), CBG+CBGA (4), Δ^9-THC+Δ^9-THCA (5), and CBD+CBDA/Δ^9-THC+Δ^9-THCA (6).
Based on the psychoactivity: ([Δ^9-THC]+[CBN]) > [CBD] (1'), ([Δ^9-THC]+[CBN]) ≈ [CBD] (2'), ([Δ^9-THC]+[CBN]) < [CBD] (3').

592

Figure 6.

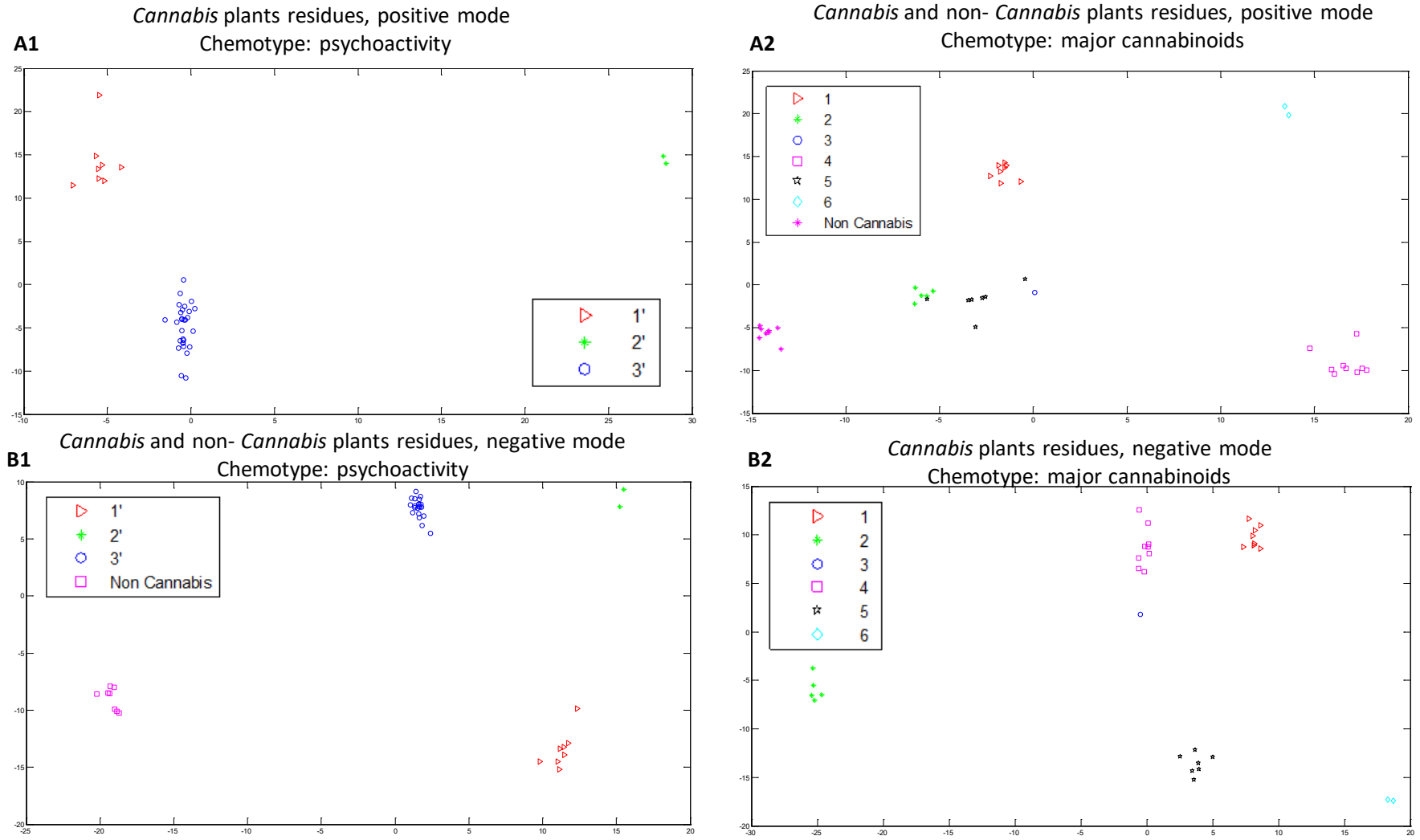
Cannabis plants residues, positive mode
Chemotype: psychoactivity
A1
1'
2'
3'
Cannabis and non- *Cannabis* plants residues, positive mode
Chemotype: major cannabinoids
A2
1
2
3
4
5
6
Non Cannabis
Cannabis and non- *Cannabis* plants residues, negative mode
Chemotype: psychoactivity
B1
1'
2'
3'
Non Cannabis
Cannabis plants residues, negative mode
Chemotype: major cannabinoids
B2
1
2
3
4
5
6

595 Table 1. Summary of the *Cannabis sativa* L. varieties studied and non-*Cannabis* plants. Based on GC-MS, *Cannabis* plants were grouped
596 according to the ratio ([Δ^9-THC]+[CBN])/[CBD]) and the main cannabinoids found, whose amount is also described.

Variety/Hybrid	**Nº of samples**	**([Δ^9-THC]+[CBN])/[CBD]**	**Chemotype (pychoactivity)[a]**	**Main cannabinoids groups**	**Amount (%, dry weight)**	**Chemotype (main cannabinoids)[b]**
C. sativa						
Theresa	1	0.04	3’	CBD+CBDA/CBDV+CBDVA	4.71/0.92	2
	2	0.05	3’	CBD+CBDA/CBDV+CBDVA	5.11/1.27	2
Pilar	1	0.07	3’	CBD+CBDA	2.11	1
	2	0.04	3’	CBD+CBDA	10.09	1
Aida	1	0.20	3’	CBG+CBGA	1.78	4
Sara	1	0.05	3’	CBD+CBDA	7.77	1
	2	0.04	3’	CBD+CBDA	11.71	1
Juani	1	0.32	3’	CBG+CBGA	1.27	4
	2	0.32	3’	CBG+CBGA	1.83	4
Octavia	1	0.23	3’	CBG+CBGA	2.10	4
Mati	1	0.69	2’	CBD+CBDA/Δ^9-THC+Δ^9-THCA	7.20/5.00	6
Moniek	1	ND[d]	1’	Δ^9-THC+Δ^9-THCA	23.50	5

597

Carma	1	0.17	3’	CBG+CBGA	1.24	4
Futura 75	1	0.05	3’	CBD+CBDA	3.42	1
	2	0.06	3’	CBD+CBDA	1.93	1
Santhica 27	1	0.25	3’	CBG+CBGA	0.93	4
Divina	1	0.05	3’	CBD+CBDA	5.04	1
Beatriz	1	0.60	2’	CBD+CBDA/Δ^9-THC+ Δ^9-THCA	7.58/4.52	6
Magda	1	415.29	1’	Δ^9-THC+Δ^9-THCA	12.05	5
H6	1	0.09	3’	CBD+CBDA/CBG+CBGA	1.04/3.07	3
H53	1	0.18	3’	CBG+CBGA	1.22	4
H6	1	0.05	3’	CBD+CBDA	6.55	1
H7	1	0.06	3’	CBD+CBDA	4.54	1
H17_p5	1	0.04	3’	CBD+CBDA/CBDV+CBDVA	5.94/1.41	2
H17_p7	1	0.04	3’	CBD+CBDA/CBDV+CBDVA	6.51/1.53	2
H17_p8	1	0.05	3’	CBD+CBDA/CBDV+CBDVA	4.52/1.11	2
H14	1	0.09	3’	CBG+CBGA	2.59	4
27/7	1	ND[d]	1’	Δ^9-THC+Δ^9-THCA	9.37	5
1 26.3/2	1	ND[d]	1’	Δ^9-THC+Δ^9-THCA	5.10	5

598

2 26.3/2	1	ND[d]	1’	Δ^9-THC+ Δ^9-THCA	5.55	5
H19	1	ND[d]	1’	CBG+CBGA	2.77	4
3 26.3/2	1	ND[d]	1’	Δ^9-THC+Δ^9-THCA	5.80	5
26.2/4	1	ND[d]	1’	Δ^9-THC+Δ^9-THCA	2.63	5
Other samples[c]						
Horsetail, aerial parts (*Equisetum arvense)*		ND[e]	-	-	-	-
Sweet chamomile, flowers (*Matricaria chamomilla*)		ND[e]	-	-	-	-
Calendula, flowers (*Calendula officinalis*)		ND[e]	-	-	-	-
Poppy, aerial parts (*Papaver rhoeas*)		ND[e]	-	-	-	-
Origanum, leaves (*Origanum vulgare*)		ND[e]	-	-	-	-
Tobacco, brand 1		ND[e]	-	-	-	-
Tobacco, brand 2		ND[e]	-	-	-	-
Aromatic pipe tobacco		ND[e]	-	-	-	-

599 [a]According to the following ratio ([Δ^9-THC]+[CBN])/[CBD]: 1’, ([Δ^9-THC]+[CBN])>[CBD]; 2’, ([Δ^9-THC]+[CBN]) ≈ [CBD]; 3’, ([Δ^9-THC]+[CBN])<[CBD]; where [Δ^9-
600 THC] is the sum of Δ^9-THCA and Δ^9-THC, CBD is the sum of CBDA and CBD.
601 [b]According to the most abundant cannabinoid groups: 1, CBD+CBDA; 2, CBD+CBDA/CBDV+CBDVA; 3, CBD+CBDA/CBG+CBGA; 4, CBG+CBGA; 5, Δ^9-THC+Δ^9-
602 THCA; 6, CBD+CBDA/Δ^9-THC+Δ^9-THCA.
603 [c]Horsetail, *Equisetum arvense*; sweet chamomile, *Matricaria chamomilla*; Calendula, *Calendula officinalis*; Poppy, *Papaver rhoeas*; Origanum, *Origanum vulgare*.
604 [d]ND, not determined because the amount of CBD+CBDA was 0%.
605 [e]These plants did not present cannabinoids (-) and so the ratio ([Δ9-THC]+[CBN])/[CBD] was not determined (ND).

606 Table 2. Main design and operating parameters of the commercial IMS device used in
607 this study.

	GDA-X
Type	Handheld
Ion source	^{63}Ni (100 MBq)
Standard inlet	Gas/vapours; thermal desorption (solids/liquids)
Drift tube temperature (ºC)	60
Standard flow of sample (mL min^{-1})	400
Drift gas flow (mL min^{-1})	200
Shutter grid type	Bradbury-Nielson
Grid pulse width/Opening time (µs)	200
Drift length (cm)	6.29
Pressure	Ambient
Inlet type	Membrane
Electric field (V cm^{-1})	289

608
609
610
611
612
613
614
615
616
617
618
619

620 Table 3. Summary of peak signals of cannabinoids standards at 100 mg L^{-1} (12 μL)

621 detected by TD-IMS**.**

Compound	Positive mode		Negative mode	
	K_0 (cm^2 V^{-1} s^{-1})[a]	Height (a.u.)	K_0 (cm^2 V^{-1} s^{-1})[a]	Height (a.u.)
Δ^9-THCA	1.842 ± 0.003 1.579 ± 0.006 1.412 ± 0.000 **1.079 ± 0.004**	55 ± 0.4 14 ± 1 13 ± 3 **27 ± 3**	**1.009 ± 0.003**	**16 ± 1**
Δ^9-THC	1.834 ± 0.004 1.568 ± 0.000 1.405 ± 0.003 **1.076 ± 0.004**[b]	44 ± 8 28 ±1 20 ± 8 **98 ± 16**	**1.008 ± 0.004**	**46 ± 8**
CBDA	**1.419 ± 0.007** **1.091 ± 0.008**	**325 ± 48** **40 ± 9**	**1.015 ± 0.000**	**23 ± 0.4**
CBD	**1.709 ± 0.011** 1.662 ± 0.004 1.584 ± 0.006 1.432 ± 0.008 **1.092 ± 0.005**[b]	**64 ± 12** 47 ± 3 40 ± 14 39 ± 2 **77 ± 42**	**1.533 ± 0.004** 1.403 ± 0.018 **1.019 ± 0.006**	**86 ± 13** 22 ± 9 **38 ± 16**
CBGA	**1.682 ± 0.001** **1.395(s)/1.420 ± 0.007/0.001** **1.096 ± 0.001** **1.044 ± 0.004**	**150 ± 16** **48 ± 5**[c] **16 ± 1** **18 ± 2**	**1.274 ± 0.006** **1.119 ± 0.001** 1.010 ± 0.003	**17 ± 9** **10 ± 4** 14 ± 1
CBG	**1.924 ± 0.015** **1.688(s)/1.737 ± 0.012/0.013** **1.410 ± 0.009** **1.102 ± 0.010** **1.048 ± 0.007**	**94 ± 15** **119 ± 11**[c] **46 ± 7** **9 ± 2** **18 ± 1**	**1.744 ± 0.005** **1.533 ± 0.008** 1.401 ± 0.004 **1.301 ± 0.006**	**18 ± 0.1** **136 ± 29** 30 ± 9 **56 ± 9**
Δ^9-THCV	1.845 ± 0.004 1.576 ± 0.002 1.400 ± 0.004 **1.162 ± 0.001**	42 ± 4 28 ± 3 18 ± 2 **198 ± 89**	**1.072 ± 0.001** **0.767 ± 0.001**	**89 ± 20** **20 ± 16**
CBDV	**1.714 ±0.005** 1.582 ± 0.007 1.429 ± 0.005 **1.182 ± 0.001**	**39 ± 10** 43 ± 12 25 ± 2 **248 ± 14**	1.883 ± 0.016 **1.732 ± 0.010** 1.589 ± 0.006 1.415 ± 0.007 **1.133 ± 0.003** **1.083 ± 0.001** **1.033 ± 0.001** **0.772 ± 0.001**	15 ± 1 **73 ± 12** 27 ± 5 16 ± 2 **77 ± 2** **88 ± 1** **24 ± 3** **32 ± 3**
Others				
CBN	1.831 ± 0.009 1.568 ± 0.001 1.404 ± 0.001 **1.090 ± 0.004**	69 ± 7 28 ± 1 20 ± 8 72 ± 29	**1.016 ± 0.004**	**34 ± 8**
Δ^8-THC	1.825 ± 0.006	52 ± 21	**1.004 ± 0.001**	**59 ± 4**

	1.565 ± 0.009 1.375 ± 0.021 **1.075 ± 0.000**	23 ± 3 15 ± 3 102 ± 11	**0.721 ± 0.002**	**13 ± 2**
CBC	1.848 ± 0.004 1.422 ± 0.001 **1.096 ± 0.002**	42 ± 10 14 ±1 88 ± 14	**1.025 ± 0.000** **0.996 ± 0.003**	**28 ± 1** **19 ± 5**

[a]Bold letter indicates more intense peaks (K_0) and/or characteristic, which may be used for differentiating them from others. (s) means shield.

[b]K_0 previously reported in literature: CBD, 1.08 $cm^2\ V^{-1}\ s^{-1}$; Δ^9-THC, 1.05-1.06 $cm^2\ V^{-1}\ s^{-1}$.

[c]Height for peak maximum.